Trade Science Inc.

April 2006 Volume 2 Issue 2

Analytical CHEMISTRY
An Indian Journal

Full Paper

ACAIJ, 2(2), 2006 [65-72]

Spectroscopic Thermodynamic Study Of The Dimerization Reaction Of Acridine Orange By Chemometrics Analysis At Different Ionic Strengths

Jahanbakhsh Ghasemi
Chemistry Department,
Faculty of Sciences, Razi University,
Kermanshah 57166 (IRAN)
Tel: +98-831-835-8077 Fax: +98-831-836-9572
E-mail: jahan.ghasemi@tataa.com

Ali Niazi[1], Alireza Nikrahi[2]
[1]Chemistry Department, Faculty of Sciences,
Azad University of Arak, Arak (IRAN)
[2]Chemistry Department, Faculty of Sciences,
Razi University, Kermanshah 57166 (IRAN)

Received: 3rd November, 2005
Accepted: 16th December, 2005
Web Publication Date: 5th April, 2006

ABSTRACT

The dimerization constants of acridine orange have been determined by studying the dependence of their absorption spectra on the temperature in the range 20-80°C at different total concentrations of acridine orange (3.3×10^{-6}-9.9×10^{-6} M) and in different ionic strengths using LiCl, NaCl and KCl inert salts. The monomer-dimer equilibrium of the acridine orange has been investigated by chemometrics refinement of the absorption spectra obtained from thermometric titrations which performed at different ionic strengths. The data processing of the undefined mixtures was performed by simultaneous resolution of the overlapping bands in the whole set of absorption spectra. The dimerization constants are varied by changing the ionic strength and the degree of dimerization are decreased by increasing of the ionic strength of the medium. Utilizing the Van't Hoff relation, which describes the dependence of the equilibrium constant on temperature, as constraint we determine the spectral responses of the monomer and dimer species as well as the enthalpy and entropy of the dimerization equilibrium. The $T\Delta S^{o}$–ΔH^{o} plot for all thermodynamic results is sketched and shows a fairly good positive correlation. The observed linear dependency indicates the enthalpy-entropy compensation in the dimerization reactions.

KEYWORDS

Dimerization;
Chemometrics;
Spectrophotometric;
Acridine orange;
Ionic strength.

INTRODUCTION

Aggregation is one of the features of dyes in solution[1-9], affecting their colouristic and photo-physical properties and therefore being of special interest. It is well known that the ionic dyes tend to aggregate in diluted solutions, leading to dimer formation, and sometimes even higher order aggregates. In such a case the molecular nature of dye is strongly affected by, and therefore related to such parameters as dye concentration and structure, ionic strength, temperature and presence of organic solvents[10]. Although dyes are very individualistic as structure and, of course behavior, certain broad rules are well established regarding the aggregation in general. It may increase with an increase of dye concentration or ionic strength; it will decrease with temperature rising or organic solvents adding; addition to the dye structure of ionic solulilizing groups will decrease aggregation, whereas the inclusion of long alkyl chains increase aggregation because of higher hydrophobic interaction in solution.

The absorption UV-Visible spectroscopy is one of the most suitable methods for quantitative studying the aggregation properties of dyes as function of concentration, since in the concentration range used (10^{-3}-10^{-6} M) mainly monomer-dimer equilibrium exists.

The dimerization of acridine orange (SCHEME I) dye is a very common phenomenon and has provided important applications in a wide range of biotechnological areas[11, 12]. Researchers have proven that acridine orange and some other fluorescent dyes form dimmers not only in aqueous solution but also in ionic surfactant solution. L.Yujing and S.Hanxi[11] reported the formation of a virtually non-fluorescent dimer of acridine orange in anionic surfactant sodium dodecyl sulfate solution. Also, the dimerization constant and absorption spectra of acridine orange dye in monomeric and dimeric form is important from the aspect of interaction by nucleic acids and used it as probe for measuring pH gradient[13,14]. In this work, we applied the physical constraints approach to determine the dimeric constants and thermodynamic parameters values of acridine orange dye in pure water and in different ionic strengthes by spectrophotometric.

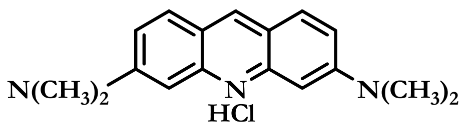

SCHEME I

Theory

Data analysis was carried out by DATAN package that developed by Kubista group. The theory and application of physical constraints method was discussed by Kubista et al. in several papers[1,15-21]. However, the general principal will be outlined briefly. Spectra of acridine orange at different temperature in range 20-80°C are digitized and arranged as rows in an n×m matrix A, where n is the number of spectra and m the number of data points in each spectra. A is decomposed into an orthogonal basis set using, for example, NIPALS[17,18]:

$$\mathbf{A} = \mathbf{TP'}+\mathbf{E} \approx \mathbf{TP'} = \sum_{i=1}^{r} t_i p_i' \tag{1}$$

where $t_i(n\times1)$ are orthogonal target vectors and $p_i'(1\times m)$ are orthogonal projection vectors. There are mathematical constructs and do not correspond to any physical property of the system. r is the number of spectroscopically distinguishable components, and E is the error matrix containing experimental noise. For a well-designed experiment, E is small compared to TP′ and can be discarded.

Assuming linear response the recorded spectra are also linear combinations of the spectra responses, $v_i(1\times m)$, of the components:

$$\mathbf{A} = \mathbf{CV} + \mathbf{E} \approx \mathbf{CV} = \sum_{i=1}^{r} c_i v_i \tag{2}$$

where $c_i(n\times1)$ are vectors containing the component concentrations at the different temperatures. The two equations are related by a rotation[18]:

$$\mathbf{X} = \mathbf{TP}^{-1} \tag{3}$$

$$\mathbf{V} = \mathbf{RP'} \tag{4}$$

where R is an r×r rotation matrix. For a two-component system:

$$R=\begin{bmatrix} r_{11} & r_{12} \\ r_{21} & r_{22} \end{bmatrix} \text{ and } R^{-1}=\frac{1}{r_{11}r_{22}-r_{12}r_{21}}\begin{bmatrix} r_{22} & -r_{12} \\ -r_{21} & r_{11} \end{bmatrix} \quad \textbf{(5)}$$

Since a single sample is studied, the total concentration must be constant, constraining matrix R[18]. For monomer-dimer equilibrium, the total concentration of monomers is constant:

$$2X \xleftrightarrow{K_D} X_2 \quad \textbf{(6)}$$

$$c_x(T)+2c_{x2}(T)=c_{tot} \text{ or } c_x+2c_{x2}=c_{tot} \quad \textbf{(7)}$$

Combining equation **(7)** with equation **(3)**, we obtain:

$$\frac{1}{r_{11}r_{22}-r_{12}r_{21}}(t_1r_{22}-t_2r_{21}-2t_1r_{12}+2t_2r_{11})=c_{tot} \quad \textbf{(8)}$$

this can be written:

$$f_{11}t_1+f_{12}t_2=c_{tot} \quad \textbf{(9)}$$

where

$$f_{11}=(r_{22}-2r_{12})(r_{11}r_{22}-r_{12}r_{21})^{-1} \quad \textbf{(10)}$$

and

$$f_{12}=(2r_{11}-r_{21})(r_{11}r_{22}-r_{12}r_{21})^{-1} \quad \textbf{(11)}$$

These can be determined, for example, by fitting the target vectors to a vector with all elements equal to c_{tot}. Equation **(10)** and **(11)** provide two relations between the elements of matrix R, hence making two of them redundant.

In most cases, the spectra of some of the components can be determined in separate measurements. For example, monomer-dimer equilibrium can, in general, be diluted sufficiently to make the dimer concentration negligible. This makes it possible to record the monomer spectrum, which, of course, should be used as a constraint in the analysis. Normalizing the monomer spectrum to the same total concentration as the analyzed sample. We obtain from equation **(4)**:

$$v_{monomer}=r_{11}p_1'+r_{12}p_2'=f_{21}p_1'+f_{22}p_2' \quad \textbf{(12)}$$

where $f_{21}=r_{11}$and $f_{22}=r_{12}$ are determined by fitting the two projection vectors to the monomer spectrum. Equation **(12)** also provides two relations between the elements of matrix R. These are not independent of equation **(9)**, and two equations cannot be combined to solve for all the elements of matrix R, but they can be used to express R in a single element, below arbitrarily chosen to be r_{21}:

$$R=\begin{bmatrix} f_{21} & f_{22} \\ r_{21} & 2f_{22}+(2f_{21}-r_{21})\frac{f_{11}}{f_{12}} \end{bmatrix} \quad \textbf{(13)}$$

Defined this way, matrix R produces C and V matrices that are consistent with the total sample concentration and the spectral response of the monomer. The value of r_{21} determines the dimer spectrum and the monomer concentration profiles.

Although value of r_{21} produces a mathematically acceptable solution, reasonable results, in terms of spectral intensities and nonnegative concentrations and spectral responses, are obtained in a relatively narrow range of r_{21} values. Still, the range is, in general, too large for a quantitative analysis.

The final constraint, which produces a unique solution, is the thermodynamic relation between temperature and the equilibrium constant. The components' concentrations are related by the law of mass action[22]:

$$K_D(T)=\frac{c_{x2}(T)/c^\circ}{(c_x(T)/c^\circ)^2} \quad \textbf{(14)}$$

where c°= 1mol/dm^3. Assuming that the dimerization constant K_D(T) depends on temperature according to the Van't Hoff equation[22],

$$\frac{d\ln K_D(T)}{d(1/T)}=-\Delta H^\circ/R \quad \textbf{(15)}$$

where ΔH° is the molar enthalpy change, R=8.31 Jmol^{-1}K^{-1} is the universal gas constant, and T is the Kelvin temperature. r_{21} can now be determined by requiring that matrix R should rotate the target vectors to give concentration vectors (equation 3) that produce an equilibrium constant whose logarithm is a linear function of 1/T. In practice, the solution is found by a simple search procedure. r_{21} is given an arbitrary value, for which a trial rotation matrix is calculated (equation 13). This is used to calculate trial concentration profiles (equation 3), which are combined to a trial equilibrium constant (equation 14). A linear regression of equilibrium constants with respect to 1/T is then performed (equation 15), which determines a trial enthalpy change of the reaction. Each trial rotation matrix also determines trial spectral responses (equation 4). The procedure repeated for various values of r_{21} to find a range that produces reasonable concentration profiles and spectral responses. This is done rather arbitrarily since there is no simple way to estimate r_{21}. Once a range has been found, r_{21} is varied gradually in this range, and a χ^2 (a regression coefficient) is calculated for each regression of $\ln K_D(T)$ with respect to $1/T$. The r_{21} that produces the best fit determines matrix R. Several studies based on the application of this method to spectrophotometric data have been reported[1,16,23-26]. The analysis is readily performed with the DATAN program version 3.1[27].

EXPERIMENTAL

Material

All the chemicals used were of analytical reagent grade. Subboiling, distilled water was used throughout. Acridine orange (for microscopy grade) was purchased from Fluka and was used without additional purification. A stock solution (1×10^{-4} M) was prepared by dissolving solid acridine orange in water. In all experiments the ionic strength was adjusted using LiCl, NaCl and KCl (Fluka) at 1.0, 2.0 and 3.0 mol l^{-1} M solutions of these salts.

Apparatus

Absorption spectra were measured on CARY 100 UV-Visible Spectrophotometer (Varian) equipment by 6×6 multi-cell and temperature controller using 1 nm bandwidth, and were digitized with five data point per nanometer. The cuvettes were treated with repel-silane prior to measurements to avoid dye adsorption.

Computer hardware and software

All absorption spectra where digitized at five data points per nanometer in the wavelength 380-550 nm and transferred (in ASCII format) to an Athlon 2000 XP computer for analysis by MATLAB (Mathworks, Version 6.5) and then processed by using DATAN package[27].

RESULTS AND DISCUSSION

The absorption spectra of acridine orange at different total dye concentrations and at different ionic strengths were recorded between 380 and 550 nm in the temperature range 20-80°C at 5°C intervals. Sample absorption spectra are shown in figure 1. As it is expected, by increasing the temperature and decreasing the concentration, the monomer form would be predominant over the dimer form. So it is wise to choose the spectrum of the dye at the highest temperature and at lowest concentration as an initial estimate for the monomer in the subsequent calculation.

According to Eqs. (1)-(15) the DATAN program start with a trial value of r_{21}, at predefined interval, and iterate all the calculation steps. The iteration stops when all r_{21} values in the initial interval are tested. The K_D, dimer spectrum and ΔH that corresponds to minimum value of χ^2 statistics, are selected as the best values. The χ^2 is a goodness of fit criterion and its value indicate the predictability of the model, i.e. how well the monomer spectrum and r_{21} are determined. The general formula of the χ^2 is;

$$\chi^2 = \sum_{i=1}^{n} (A_{\exp} - A_{calc})^2 / A_{\exp} \qquad \textbf{(16)}$$

where $\mathbf{A}_{\exp}$ is the expected value and $\mathbf{A}_{calc}$ is calculated from experimental data over n data points.

With increasing temperature the absorption peaks around 490 nm grows and at the around 470 nm decrease (Figure 1). We analyzed the temperature titrations by assuming the monomer-dimer, monomer-dimer-trimer, and even models including higher order aggregates, and it's observed that just the monomer-dimer model habitually describes the data. The presence of exactly two species is also evidenced by the isobestic point at 474 nm.

The dimerization constant (K_D) was calculated at different temperatures at the four total dye concentrations (TABLE 1). From the dependence of

TABLE 1: Dimeric constant ($\log K_D$) and thermodynamic parameters values of acridine orange dye at different concentrations without adjusting ionic strength in water.

Concentartion (mol l^{-1})	3.3×10^{-6}	6.6×10^{-6}	9.9×10^{-6}	1.32×10^{-5}
$\log K_D$ (25°C)	6.46	6.13	5.96	5.78
ΔH° (kJ mol^{-1})	-96.6	-95.8	-94.7	-92.6
ΔS° (J mol^{-1} K^{-1})	-201.9	-204.7	-204.6	-200.6

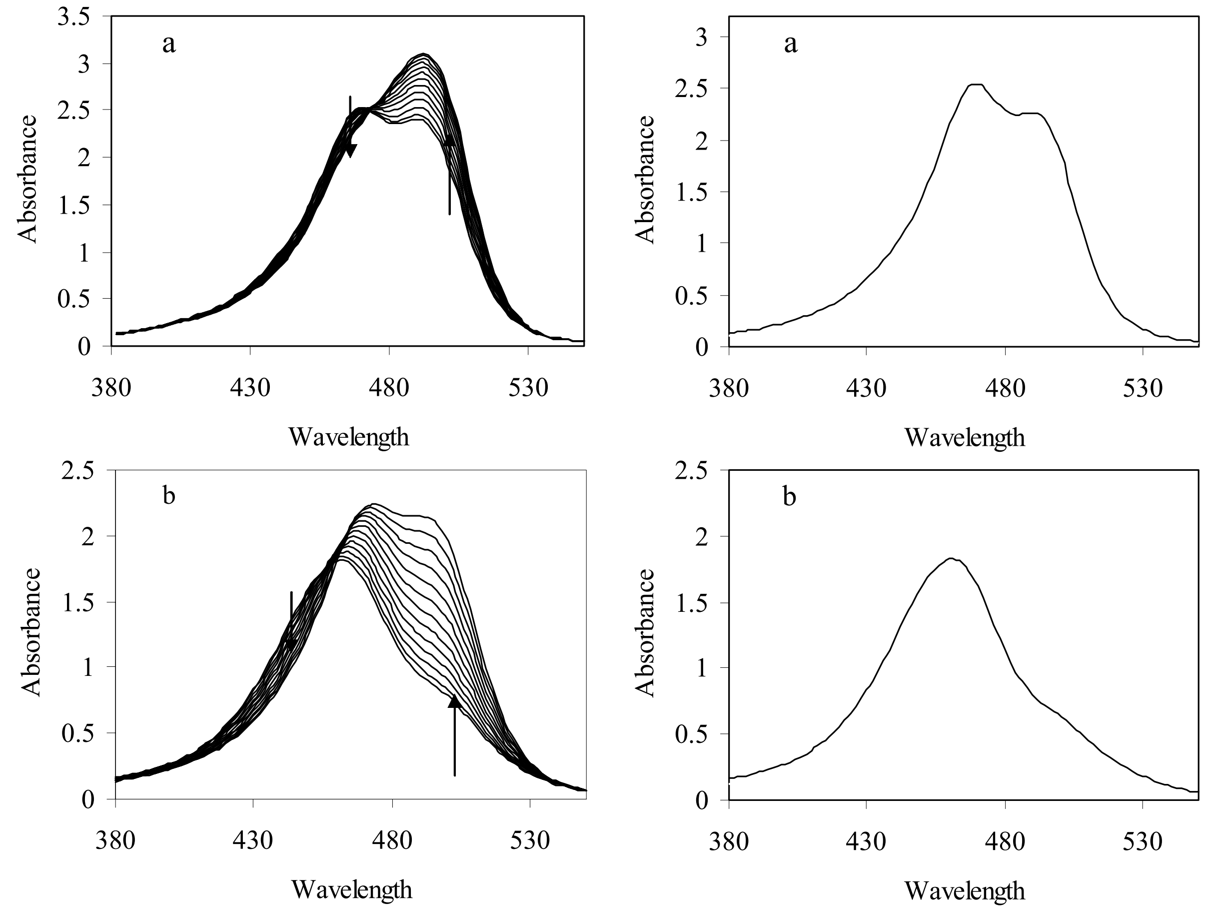

Figure 1: Absorption spectra and calculated absorption spectra of monomer (—) and dimer (—) of acridine orange dye (9.9×10^{-6} M) in 5°C intervals between 20- 80°C (a: in water, b: 3 M NaCl).

$\ln K_D$ on 1/T (Figure 2) ΔH° and ΔS° values were determined (TABLE 1). The ΔH° values ranges from –92.6 to -96.6 $kJmol^{-1}$ with mean -94.9, while ΔS° ranges from -200.6 to -204.7 $Jmol^{-1}K^{-1}$ with mean -203.0 $Jmol^{-1}K^{-1}$. This relationship between entropy and enthalpy reflects the electrostatic nature of the dimerization phenomenon. The variations of the monomer and dimer form concentrations of acridine orange with temperature is shown in figure 3. The sample calculated absorption spectra of acridine orange dye in monomer and dimer forms are shown in figure 1. The spectrum of the monomer has maximum intensity at 490 nm. It is very similar to the spectrum measured in dilute solution at high temperature that was used as initial estimate. The dimer spectrum has maximum at 470 nm.

For studying the effect of ionic strength on dimerization of acridine orange, the inert salts, lithium chloride, sodium chloride and potassium chloride, were selected and dimerization was investigated. The sample absorption spectra of acridine orange (9.9×10^{-6} M) at ionic strength in 3 mmol ml^{-1} of sodium chloride in the temperature range 20-80°C at 5°C intervals is shown in figure 1. The dimerization constants (K_D) was calculated at different temperatures and at three ionic strengths (TABLE 2). The dimeric constant at 25°C and thermodynamic parameters values of acridine orange at different ionic strengths, made by lithium chloride, sodium chloride and potassium chloride, are listed in TABLE 2. The sample calculated absorption spectra of monomer and dimer forms of acridine orange at ionic strength in 3 mmol ml^{-1} of sodium chloride is also shown in figure 1.

According to extended Debye-Huckel equation[28-30], the change of the ionic strength and its ac-

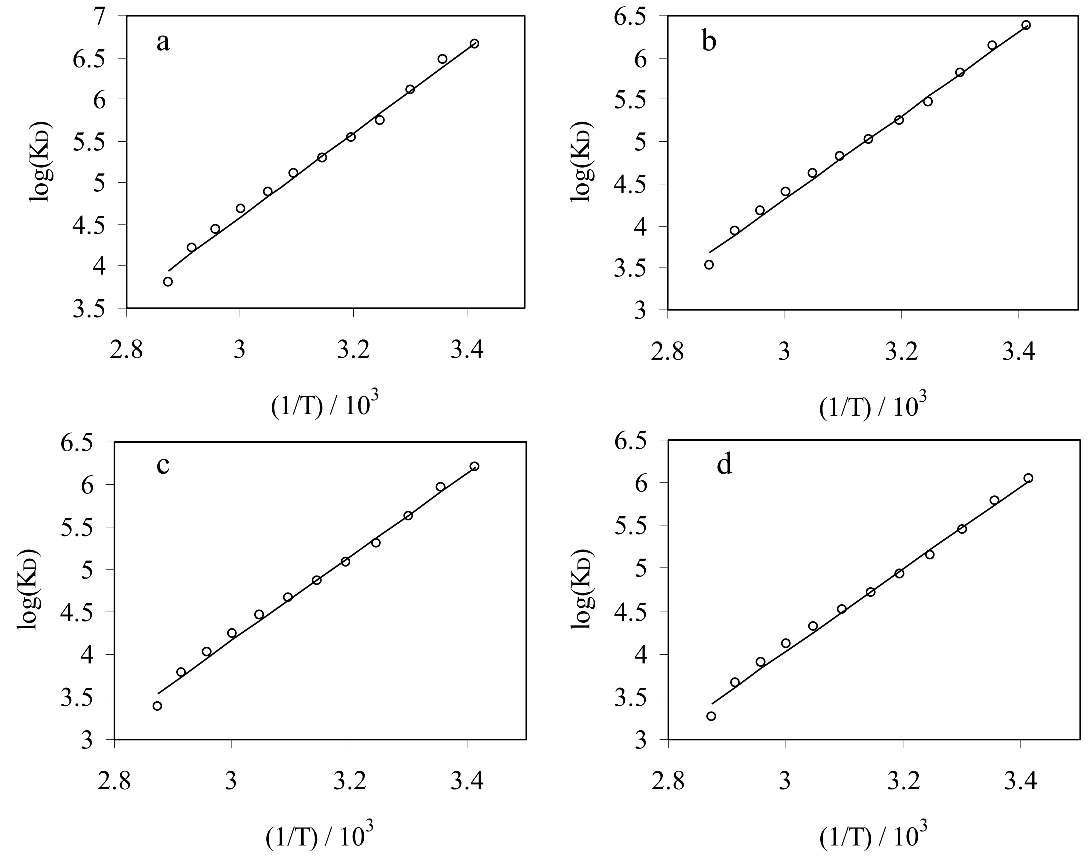

Figure 2: The Van't Hoff equation plot at different concentrations of acridine orange dye (a: 3.3×10^{-6}, b: 6.6×10^{-6}, c: 9.9×10^{-6}, d: 1.32×10^{-5} M).

TABLE 2: Dimeric constant ($\log K_D$) and thermodynamic values of acridine orange dye at different salts.

	c(Salt) (mol l^{-1})	1	2	3
LiCl	$\log K_D$ (25°C)	6.58	6.67	6.46
	ΔH° (kJ mol^{-1})	-106.4	-108.1	-102.1
	ΔS° (J mol^{-1} K^{-1})	-233	-237	-219
NaCl	$\log K_D$ (25°C)	6.40	6.44	6.37
	ΔH° (kJ mol^{-1})	-102.9	-103.3	-98.8
	ΔS° (J mol^{-1} K^{-1})	-223	-224	-209
KCl	$\log K_D$ (25°C)	6.47	6.79	6.90
	ΔH° (kJ mol^{-1})	-96.7	-106.5	-111.2
	ΔS° (J mol^{-1} K^{-1})	-202	-230	-243

companying effect on the dimerization constants is totally depend on the relative changing of the total charge of the dimer species with respect to the two monomer moieties. As it can be seen from the spectral data obtained at different ionic strength, the increasing of the ionic strength apparently produce more dimer, as the absorption spectrum recorded at high ionic strength is more similar to the dimer form than the monomer form. But indeed, the addition of all of these solutes and consequently the increasing of ionic strength are reduced the dimer formation and in turn the dimerization constants(TABLE 1 and 2). As it can be seen from the spectral data obtained at different ionic strengths, the increasing of the ionic strength affects the dimerization process and all the solutes decrease the dimerization constants. The comparison of the spectral data shown in figure 1 and data presented in TABLE 1 and TABLE 2 clearly verify these findings.

Despite the above mentioned variations which has deterministic effect on the thermodynamics parameters of dimerization of acridine orange, the TΔS versus ΔH° plot of the shows a fairly good linear correlation (Figure 4) indicating the existence of enthalpy-entropy compensation in the dimeric reactions. The linear correlation observed between TΔS

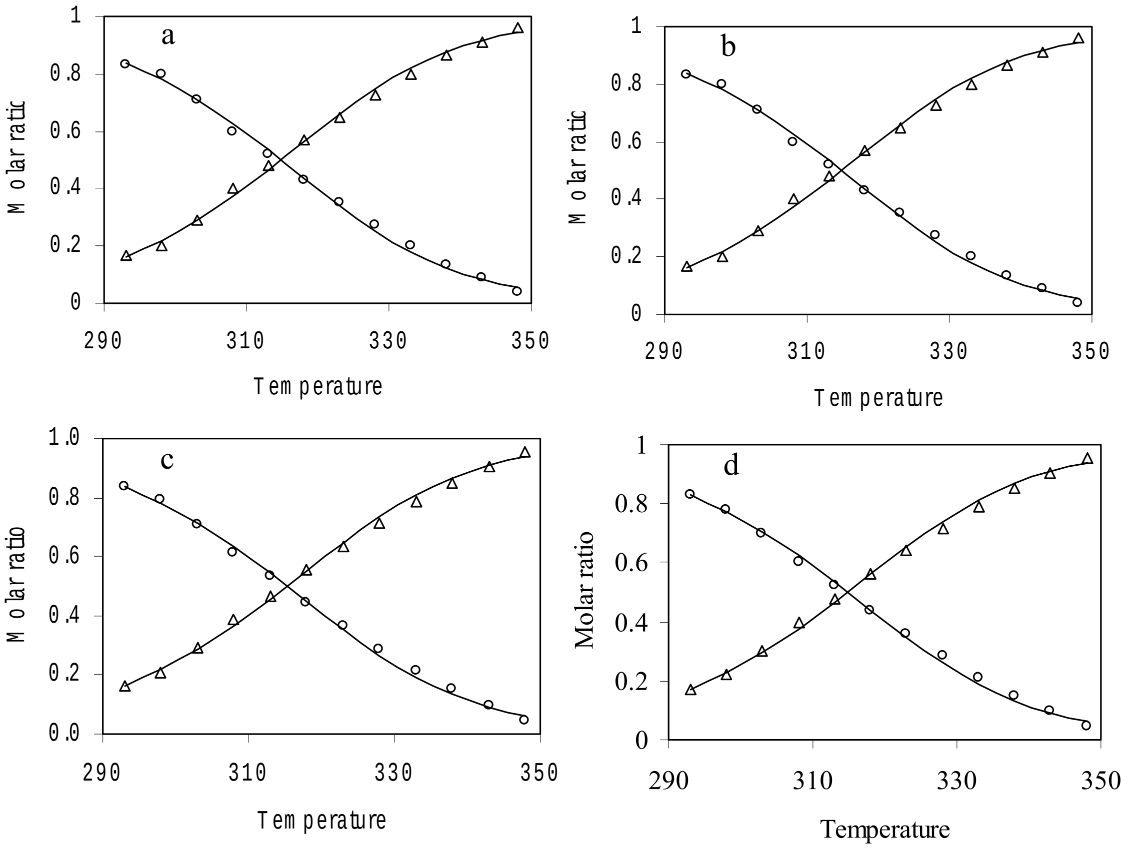

Figure 3: Molar ratio of acridine orange dye monomer (∆) and dimer (o), compared to molar ratios predicted by the temperature dependence of the equilibrium constants (shown as line) at different concentrations of acridine orange dye in water (a: 3.3×10^{-6}, b: 6.6×10^{-6}, c: 9.9×10^{-6}, d: 1.32×10^{-5} M).

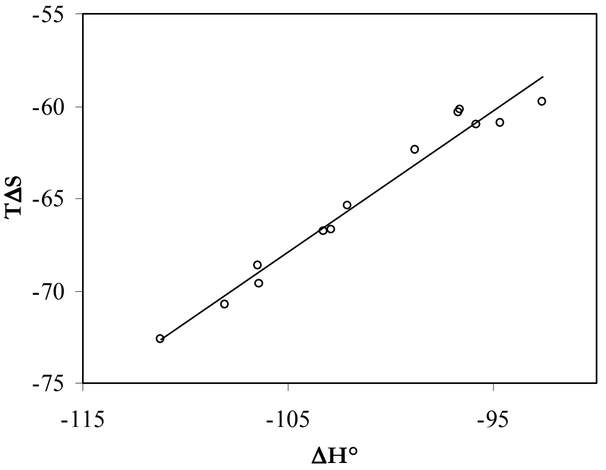

Figure 4: Plot of T∆S versus ∆H° for dimerization of acridine orange at different concentrations in various ionic strengths.

and ΔH° values can be expressed as $T\Delta S = T\Delta S^\circ + \alpha\Delta H^\circ$ with $T\Delta S^\circ = 12.4$ kJ mol^{-1}, $\alpha = 0.7653$ ($R^2 = 0.969$) for thermodynamics data of dimerization process of acridine orange dye. The same trends are reported form the thermodynamics study of the reactions with largely accompanying with changing in electrostatic interactions during the association reactions or host-guest phenomena[31,32].

The result suggests that the entropic effect consists of two components. The first component $T\Delta S^\circ$ in independent of enthalpy change and the second is proportional to it. The proportionality constant α might be considered a quantitative measure of the enthalpy-entropy compensation. For acridine orange, $\alpha = 0.7653$, about 24% of the increase in ΔH contributed to dimeric stability. The close to zero intercept of $T\Delta S^\circ = 12.4$ kJ mol^{-1} reveals that the dimerization process here, in nature are can be classified as enthalpy driven. This results can be supported by the fact that the dimerization constants is increased by increasing of the ionic strengths of the medium which in turn show the increasing of the charge of the dimer are more solvated by the solvents molecules and entropic change would have less positive values.

CONCLUSION

In this study we report a method for characterization of monomer-dimer equilibrium of acridine orange dye at different ionic strength. We determine the dimeric constant, concentration profiles for the monomer and dimer, and spectral responses of monomer and dimer. The thermodynamic parameters of dimerization reaction were calculated from the dependence of dimeric constant on the temperature (Van't Hoff equation). The relationship between entropy and enthalpy reflects the electrostatic nature of the dimerization phenomenon, which can be quantitatively expressed in the relation of $T\Delta S^{o}$–ΔH^{o} and also show the dimerization reaction in this case are classified in the enthalpy driven category of reactions.

REFERENCES

[1] J.Ghasemi, A.Niazi, G.Westman, M.Kubista; Talanta, **62**, 835 **(2004)**.

[2] N.O.Mchedlov-Petrosyan, Y.V.Kholin; Russian J.of Applied.Chem., **77**, 414 **(2004)**.

[3] N.O.Mchedloy-Petrossyan,V.I.Kukhtik, V.I.Alekseeva; Dyes Pigments, **24**, 11-35 **(1994)**.

[4] N.O.Mchedloy-Petrossyan, V.I.Kukhtik, V.D.Bezugliyz; J.Phys.Org.Chem., **16**, 380-397 **(2003)**.

[5] N.O.Mchedloy-Petrossyan, N.A.Vodolazkaya, A.O. Doroshenko; J.Fluorescence, **13**, 235-248 **(2003)**.

[6] L.Antonov, G.Gergov, V.Petrov, M.Kubista, J.Nygren; Talanta, **49**, 99 **(1999)**.

[7] L.Evans III, G.Patonay; Talanta, **48**, 933 **(1999)**.

[8] G.J.Su, S.X.Yin, L.J.Wan, J.C.Zhao, C.L.Bai; Surface Sci., **551**, 204 **(2004)**.

[9] A.K.Chibisov, V.I.Prokhorenko, H.Gorner; Chem. Phys., **250**, 47 **(1999)**.

[10] B.C.Burdett; 'Aggregation of dyes, In studies in Physical and Theoretical Chemistry', Elsevier, 2 **(1983)**.

[11] L.Yujing, S.Hanxi; Anal.Commun., **36**, 135 **(1999)**.

[12] A.P.Wei, D.K.Blumental, J.N.Herron; Anal.Chem., **66**, 1500 **(1994)**.

[13] J.Kapuscinski, Z.Darzynkiewicz; J.Biomol.Struct.Dyn., **5**, 127 **(1987)**.

[14] M.G.Palmgren; Anal.Biochem., **192**, 316 **(1991)**.

[15] M.Kubista, R.Sjoback, J.Nygren; Anal.Chim.Acta, **302**, 121 **(1995)**.

[16] J.Ghasemi, A.Niazi, M.Kubista, A.Elbergali; Anal. Chim.Acta, **455**, 335 **(2002)**.

[17] M.Kubista, J.Nygren, A.Elbergali, R.Sjoback; Crit.Rev. in Anal.Chem., **29**, 1 **(1999)**.

[18] M.Kubista, R.Sjoback, B.Albinsson; Anal.Chem., **65**, 994 **(1993)**.

[19] Scarminio, M.Kubista; Anal.Chem., **65**, 409 **(1993)**.

[20] Elbergali, J.Nygren, M.Kubista; Anal.Chim.Acta, **379**, 143 **(1999)**.

[21] J.Nygren, J.M.Andrade, M.Kubista; Anal.Chem., **68**, 1706 **(1996)**.

[22] L.V.Levine; 'Physical Chemistry', McGraw-Hill, New York **(1988)**.

[23] N.Svanvik, J.Nygren, G.Westman, M.Kubista; J.Am. Chem.Soc., **123**, 803 **(2001)**.

[24] J.Nygren, N.Svanvik, M.Kubista; Biopolymers, **46**, 39 **(1998)**.

[25] J.Nygren, A.Elbergali, M.Kubista; Anal.Chem., **70**, 4841 **(1998)**.

[26] J.Ghasemi, Sh.Ahmadi, M.Kubista, A.Forootan; J. Chem.Eng.Data, **48**, 1178 **(2003)**.

[27] http://www.multid.se.

[28] P.Debye, E.Huckel; Phys.Z., **24**, 165 **(1923)**.

[29] P.Debye, E.Huckel; Phys.Z., **24**, 305 **(1923)**.

[30] H.A.Laitinen, W.E.Harris; 'Chemical Analysis', McGraw Hill, London **(1975)**.

[31] J.Ghasemi, M.Shamsipur; J.Coord.Chem., **36**, 183-194 **(1995)**.

[32] J.Ghasemi, Z.A.Meibody; J.Sci.Iran, **10**, 158-164 **(1999)**.